

Supporting Information for

Functionalizing Tetraphenylpyrazine With Perylene Diimides (PDIs) As High-Performance Nonfullerene Acceptors

Gang Li^{a‡}, Shufan Yang^{a‡}, Tao Liu^{ab*}, Jiwei Li^c, Wenbin Yang^a, Zhenghui Luo^b, Cenqi Yan^a, Dandan Li^a, Xinyu Wang^a, Guanwei Cui^a, Tao Yang^d, Liang Xu^e, Shun-Ze Zhan^e, Lijun Huo^f, He Yan^{b*} and Bo Tang^{a*}*

^a College of Chemistry, Chemical Engineering and Materials Science, Key Laboratory of Molecular and Nano Probes, Ministry of Education, Collaborative Innovation Center of Functionalized Probes for Chemical Imaging in Universities of Shandong, Institute of Materials and Clean Energy, Shandong Provincial Key Laboratory of Clean Production of Fine Chemicals, Shandong Normal University, Jinan 250014, P. R. China.

^b Department of Chemistry and Hong Kong Branch of Chinese National Engineering Research Center for Tissue Restoration & Reconstruction, Hong Kong University of Science and Technology, Clear Water Bay, Kowloon, Hong Kong

^c Key Laboratory of Flexible Electronics (KLOFE) & Institute of Advanced Materials (IAM), Jiangsu National Synergetic Innovation Center for Advanced Materials (SICAM); Nanjing Tech University (NanjingTech), 30 South Puzhu Road, Nanjing, 211816, P.R. China.

^d Key Laboratory of Biofuels, Qingdao Institute of Bioenergy and Bioprocess Technology, Chinese Academy of Sciences, P. R.China

^e Key Laboratory for Preparation and Application of Ordered Structural Materials of Guangdong Province, Shantou University, Shantou 515063, P. R. China.

^f School of Chemistry, Beihang University, Beijing 100191, P. R. China

‡These authors contributed equally to this work.

Corresponding E-mail:

ligang@sdnu.edu.cn

liutaozhx@ust.hk

hyan@ust.hk

huolijun@buaa.edu.cn

tangb@sdnu.edu.cn

1. Materials and Measurements

All solvents and reagents were used as received from commercial sources and used without further purification unless otherwise specified. Compounds 1,2-bis(4-bromophenyl)-2-hydroxyethanone (**2**)¹, 2,3,5,6-tetrakis(4-bromophenyl)pyrazine (**3**)² and 2,3,5,6-tetrakis(4-(4,4,5,5-tetramethyl-1,3,2-dioxaborolan-2-yl)phenyl)pyrazine (**TPP-Bpin4**)² were synthesized according to the reported literature. **PDBT-T1** was synthesized according to our published paper,³ Weight average molecular weight (M_w) and polydispersity index (PDI) estimated from GPC are 342kDa and 1.75, respectively. ¹H NMR (400 MHz) and ¹³C NMR (100 MHz) spectra were measured on a Bruker 400 MHz spectrometer. UV-vis-NIR absorption spectra were recorded on a Shimadzu UV-2700 recording spectrophotometer. Cyclic voltammetry (CV) measurements were carried out on a CHI660E voltammetric analyzer at room temperature. Tetrabutylammonium hexafluorophosphate (*n*-Bu₄NPF₆, 0.1 M) was used as the supporting electrolyte. The conventional three-electrode configuration consists of a platinum working electrode with a 2 mm diameter, a platinum wire counter electrode, and an Ag/AgCl wire reference electrode. Cyclic voltammograms were obtained at a scan rate of 100 mV/s. The film morphology was measured using an atomic force microscope (AFM, Bruker-ICON2-SYS) using the tapping mode. The RMS values of the surface AFM images are averaged based on five times testing on different areas for each sample. DFT calculations were performed by using Gaussian at the B3LYP/6-31G (d, p) level, and the long alkyl chain was simplified as methyl. Thermogravimetric analysis (TGA) was carried out on a TA Instrument TA Q50 Thermogravimetric Analyzer at a heating rate of 10 °C/min up to 600 °C.

2. Space charge-limited current (SCLC) device fabrication

The structure of electron-only devices is ITO/ZnO/active layer/ZrAcAc/Al and the structure of hole-only devices is ITO/MoO_x/active layers/MoO_x/Al. The fabrication conditions of the active layer films are same with those for the solar cells. The charge mobilities are generally described by the Mott-Gurney equation:

$$J = \frac{9}{8} \varepsilon_r \varepsilon_0 \mu \frac{V^2}{L^3}$$

where J is the current density, ε_0 is the permittivity of free space (8.85×10^{-14} F/cm), ε_r is the dielectric constant of used materials, μ is the charge mobility, V is the applied voltage and L is the active layer thickness. The ε_r parameter is assumed to be 3, which is a typical value for organic materials. In organic materials, charge mobility is usually field dependent and can be

described by the disorder formalism, typically varying with electric field, $E=V/L$, according to the equation:

$$\mu = \mu_0 \exp\left[-0.89\gamma \sqrt{\frac{V}{L}}\right]$$

Where μ_0 is the charge mobility at zero electric field and γ is a constant. Then, the Mott-Gurney equation can be described by:

$$J = \frac{9}{8} \epsilon_r \epsilon_0 \mu_0 \frac{V^2}{L^3} \exp\left[-0.89\gamma \sqrt{\frac{V}{L}}\right]$$

3. Film and Device Characterization

The ultraviolet-visible (UV-Vis) absorption spectra of neat and blend films were obtained using a Shimadzu UV-2700 PC spectrometer. The current-voltage (I - V) curves of all OSCs were measured in a high-purity nitrogen-filled glove box using a Keithley 2400 source meter. AM 1.5G irradiation at 100 mW/cm² provided by An XES-40S2 (SAN-EI Electric Co., Ltd.) solar simulator (Class AAA solar simulator, Model 94063A, Oriel), which was calibrated by a standard Si diode (with KG5 filter, purchased from PV Measurement to bring spectral mismatch to unity). EQEs were measured using an Enlitech QE-S EQE system equipped with a standard Si diode. Monochromatic light was generated from a Newport 300W lamp source. The morphology of the active layers was investigated by atomic force microscopy (AFM) using a Dimension Icon AFM (Bruker-ICON2-SYS) in a tapping mode.

4. Electrochemical Characterization

Electrochemical measurements were performed under nitrogen in deoxygenated 0.1 M solutions of tetra-n-butylammonium hexafluorophosphate in dry dichloromethane using a CHI 660E electrochemical workstation, a glassy carbon working electrode, a platinum wire auxiliary electrode, and an Ag/AgCl reference electrode. Cyclic voltammograms were recorded at a scan rate of 100 mV s⁻¹. The lowest unoccupied molecular orbital (LUMO) levels were estimated based on the onset reduction potential (E_{red}), and the reduction potential was calibrated using ferrocene ($E_{\text{Fc}/\text{Fc}^+}$) as a reference ($E_{\text{red}} = -[E_{\text{measured}} - E_{\text{Fc}/\text{Fc}^+} + 4.80]$ eV).

5. AFM Characterization.

AFM measurements were performed by using a Dimension Icon AFM (Bruker). All films were coated on ITO glass substrates.

6. Computational Studies

The geometry was optimized by density functional theory (DFT) using the B3LYP hybrid functional with basis set B3LYP/6-31G(d, p).⁴ Quantum chemical calculation was performed with the Gaussian 09 package. The long alkyl chains were replaced with an isopropyl group for simplification.

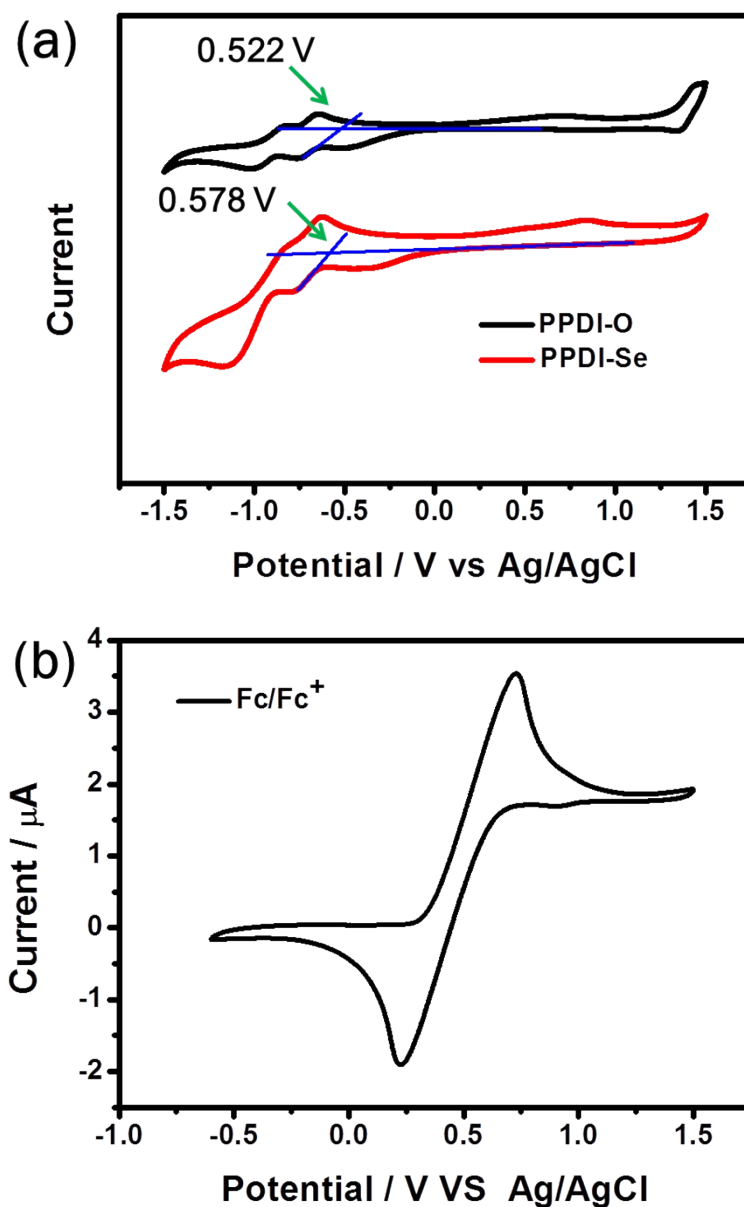


Figure S1. (a) CV curves of PPDI-O and PPDI-Se. (b) CV curve of ferrocene.

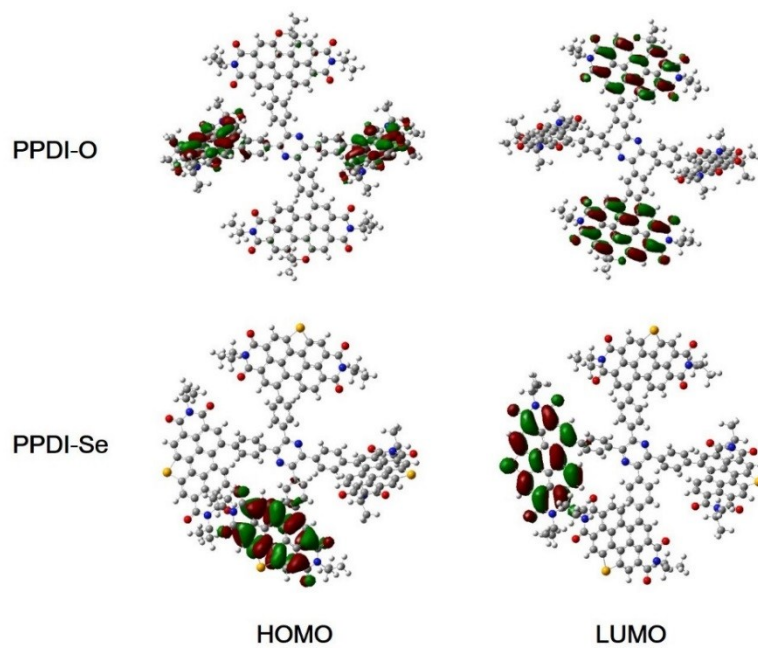


Figure S2. Wave function of PPDI-O and PPDI-Se simulated with B3LYP/6-31G(d, p) level.

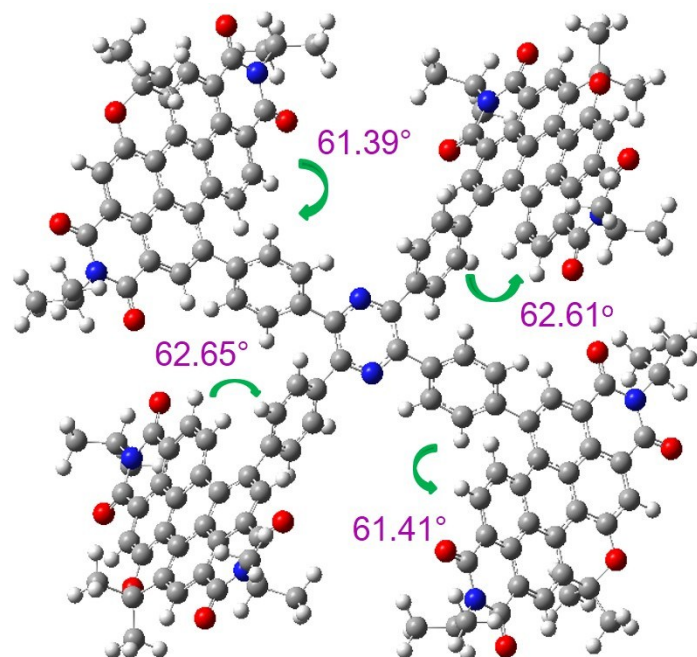


Figure S3. Optimized molecular geometries of PPDI-O at B3LYP/6-31G(d, p).

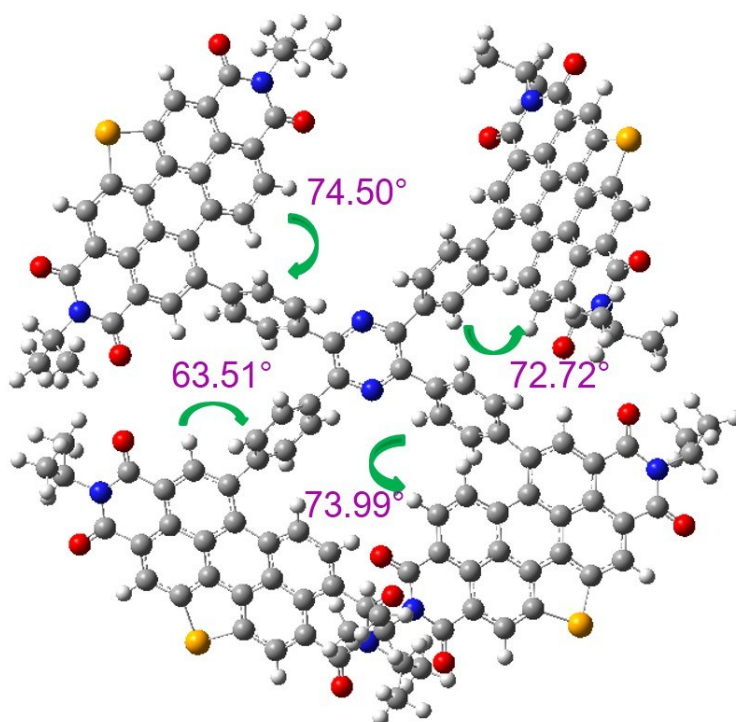


Figure S4. Optimized molecular geometries of PPDI-Se at B3LYP/6-31G(d, p).

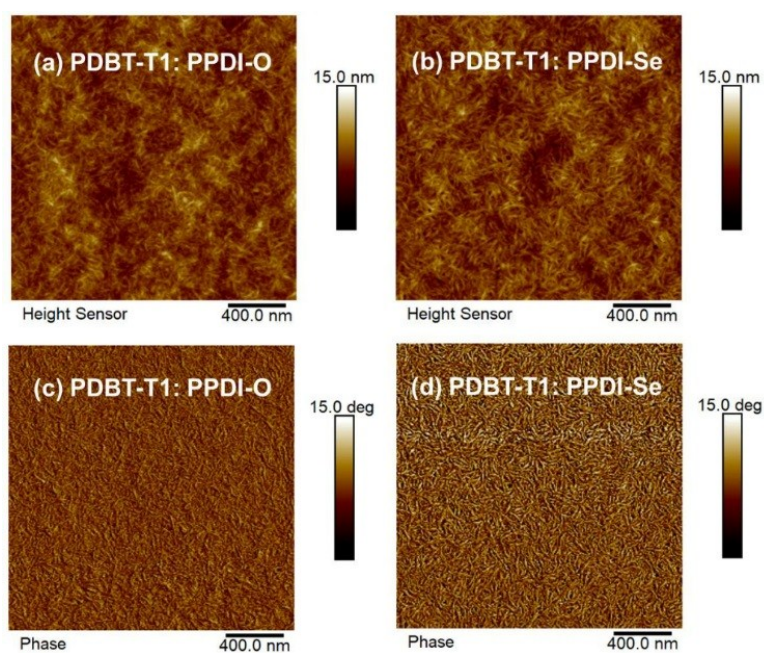


Figure S5. Film morphology images, AFM height and phase images of blend films. a, c) PDBT-T1: PPDI-O, RMS = 1.01 nm; b, d) PDBT-T1: PPDI-Se, RMS = 1.07 nm.

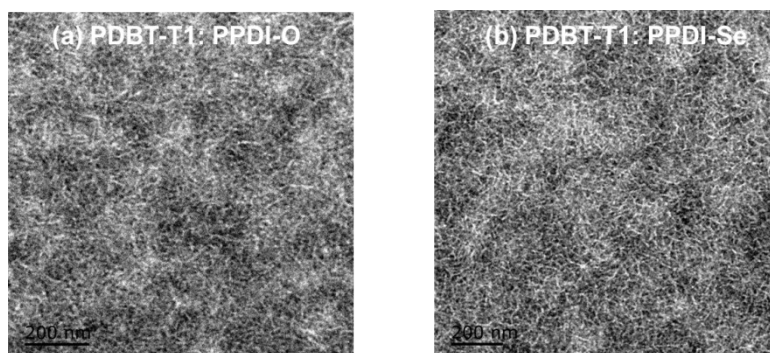


Figure S6. TEM images of a) PDBT-T1: PPDI-O and b) PDBT-T1: PPDI-Se.

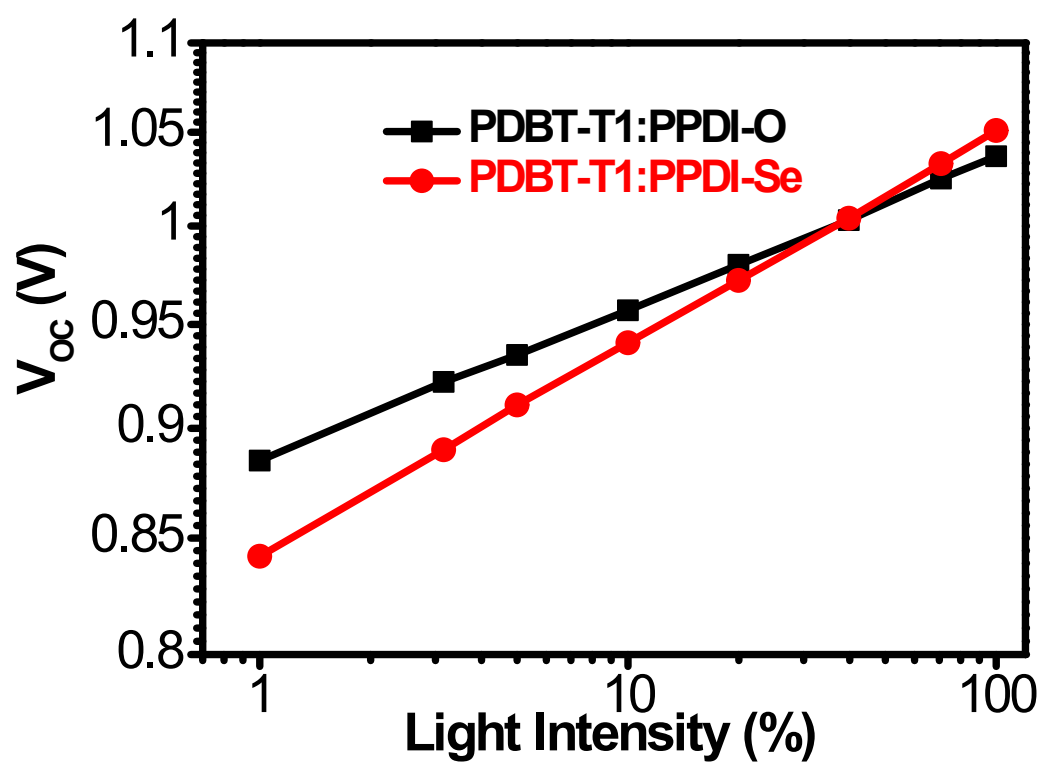


Figure S7. Light intensity dependence of V_{oc} .

Table S1. The calculated data of PPDI-O and PPDI-Se.

Samples	HOMO	LUMO	E_g
PPDI-O	-5.87	-3.55	2.32
PPDI-Se	-6.13	-3.59	2.54

Table S2. Hole and electron mobility of as-synthesized acceptors and blend films.

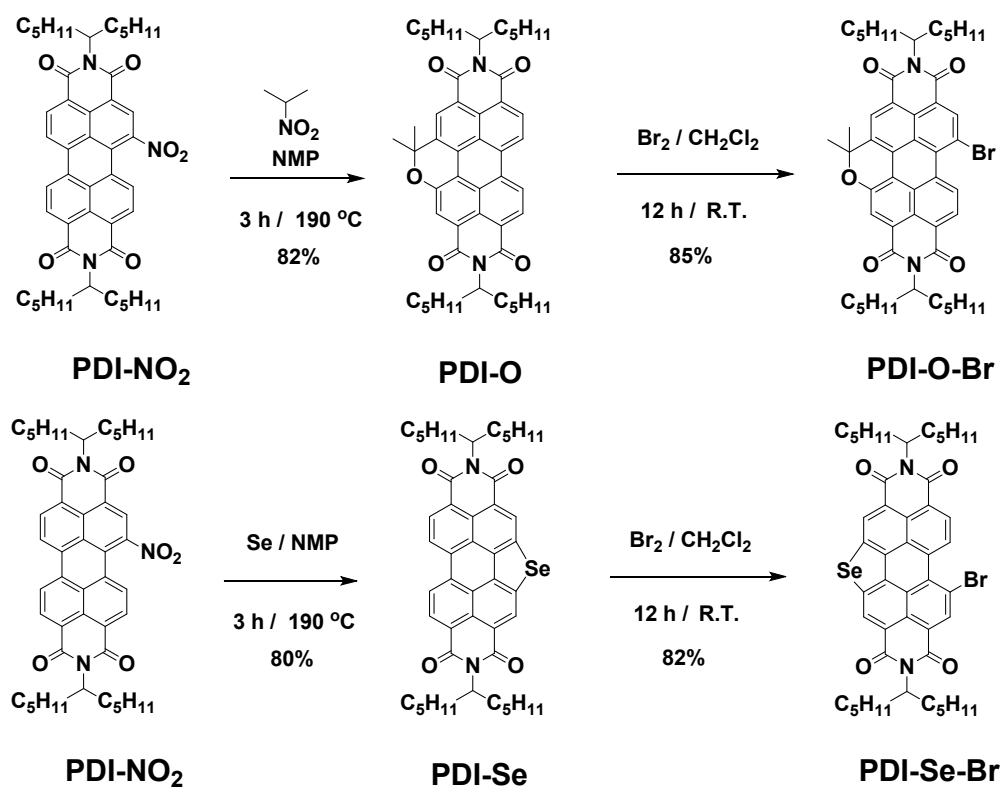
Samples	Hole mobility ($\text{cm}^2 \text{V}^{-1} \text{s}^{-1}$)	electron mobility ($\text{cm}^2 \text{V}^{-1} \text{s}^{-1}$)
PDBT-T1: PPDI-O	6.24×10^{-4}	2.78×10^{-4}
PDBT-T1: PPDI-Se	6.51×10^{-4}	3.40×10^{-4}
PPDI-O	-	5.32×10^{-4}
PPDI-Se	-	6.57×10^{-4}

Table S3. Key photovoltaic parameters calculated from the $J_{\text{ph}}-V_{\text{eff}}$ curves of PDBT-T1: PPDI-O and PDBT-T1: PPDI-Se based devices after annealing.

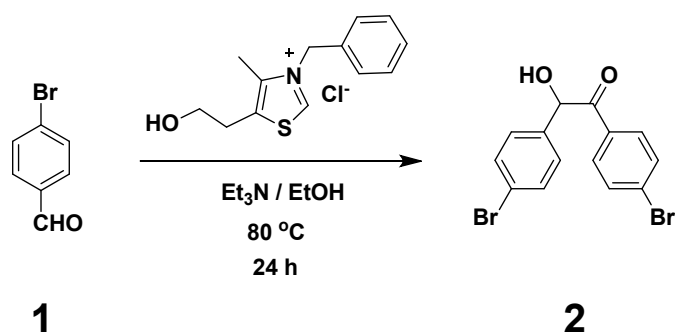
Samples	$J_{\text{sat}}^{\text{a}}$ (mA.cm^{-2})	J_{ph}^{b} (mA.cm^{-2})	J_{ph}^{c} (mA.cm^{-2})	$J_{\text{ph}}^{\text{b}}/J_{\text{sat}}$ (%)	$J_{\text{ph}}^{\text{c}}/J_{\text{sat}}$ (%)
PDBT-T1: PPDI-O	10.4	8.51	5.2	81.7	50.7
PDBT-T1: PPDI-Se	11.9	10.7	8.89	89.5	74.2

^aThe J_{ph} under condition of $V_{\text{eff}} = 3.0 \text{ V}$; ^bThe J_{ph} under short circuit condition; ^cThe J_{ph} under maximum power output condition.

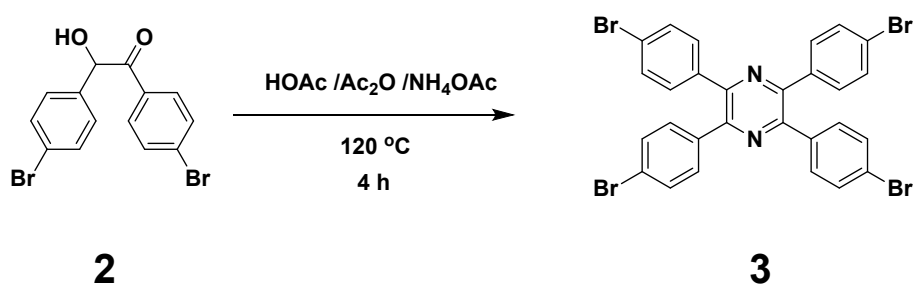
7. Synthetic routes of PDI-Se-Br and PDI-O-Br.



8. Synthetic details.

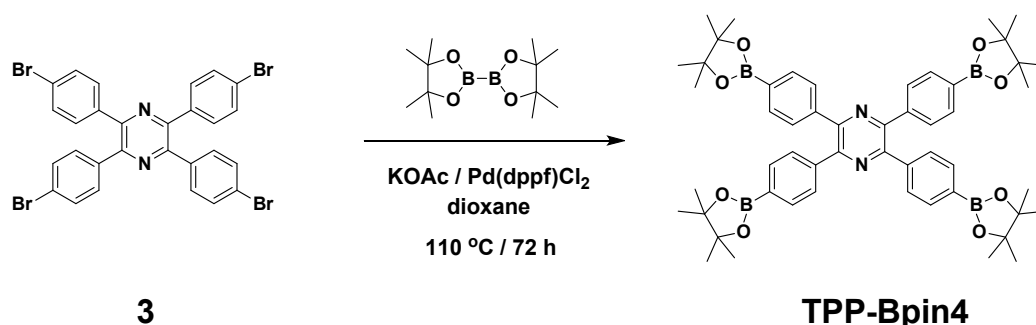


1,2-bis(4-bromophenyl)-2-hydroxyethanone (2). The reactions were carried out as literature with a little modification: An oven-dried 100 mL Schlenk tube equipped with a magnetic stir bar was charged with 4-Bromobenzaldehyde (5.55 g, 30 mmol) and 3-Benzyl-5-(2-hydroxyethyl)-4-methylthiazolium chloride (405 mg, 1.5 mmol) in 20 mL of ethanol, and then sealed tightly with a rubber septum. The tube was evacuated and backfilled with argon three times. Et₃N (1.5 ml, 10.8 mmol) was added via a syringe. The mixture was stirred for 24 h at 80 °C under N₂. After the reaction was completed, the mixture was concentrated and extracted with dichloromethane (3×50 mL), washed with water and brine three times, and then dried with anhydrous Na₂SO₄. The solvent was removed under reduced pressure. The residue was purified by silica gel chromatography eluting with petroleum ether / dichloromethane (1:2) to give the light yellow solid (2.1 g, 37.8 % yield). ¹H NMR (400 MHz, CDCl₃) δ 7.77 (d, 2H), 7.58 (d, 2H), 7.48 (d, 2H), 7.21 (d, 2H), 5.89 (d, 1H), 4.53 (d, 1H).



2,3,5,6-tetrakis(4-bromophenyl)pyrazine (3). To a 100 mL Schlenk tube were added compound **2** (1.0 g, 2.70 mmol), NH₄OAc (625 mg, 8.11 mmol) and protected with nitrogen. Acetic acid (3 mL) and acetic anhydride (0.38 mL, 4.05 mmol) were added through syringe. Then the solution was heated at 120 °C for 4 h with stirring. After cooled to room temperature, the solution was filtered and the residue was washed with a small amount of acetic acid. The product was obtained without further purification as yellow powder **3** (235 mg, 25% yield).

^1H NMR (400 MHz, CDCl_3) δ 7.49 (s, 16H). ^{13}C NMR (100 MHz, CDCl_3) δ 147.73, 137.00, 132.09, 131.68, 124.03.



2,3,5,6-tetrakis(4-(4,4,5,5-tetramethyl-1,3,2-dioxaborolan-2-yl)phenyl)pyrazine (TPP-Bpin4). To a 20 mL Schlenk tube were quickly added compound **3** (200 mg, 0.285 mmol), bis(pinacolato)diboron (297 mg, 1.17 mmol), potassium acetate (229 mg, 2.34 mmol) and $\text{Pd}(\text{dppf})\text{Cl}_2 \cdot \text{DCM}$ (23 mg, 0.0285 mmol) and protected with nitrogen. Dioxane (10 mL) was added and the solution is heated at 85 °C for 48 h with stirring. After cooled to room temperature, the reaction mixture was diluted with chloroform and washed with water and brine. The organic layer was dried over Na_2SO_4 , filtered and concentrated. Then the residue was purified through a short silica gel column with CH_2Cl_2 : ethyl acetate (5:1) to give pure product as white powder (150 mg, 59% yield). ^1H NMR (400 MHz, CDCl_3) δ 7.73 (d, 8H), 7.61 (d, 8H), 1.35 (s, 48H).

9. Spectroscopic data

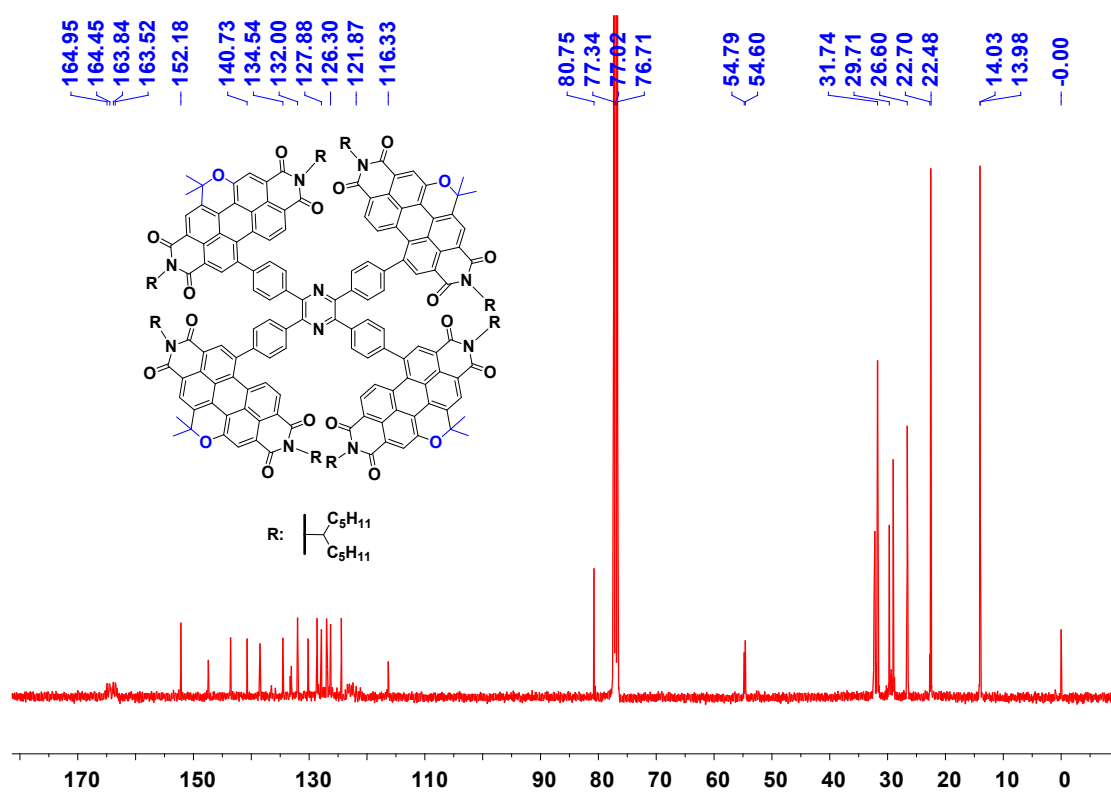


Figure S10. ^{13}C NMR spectrum of PPDI-O.

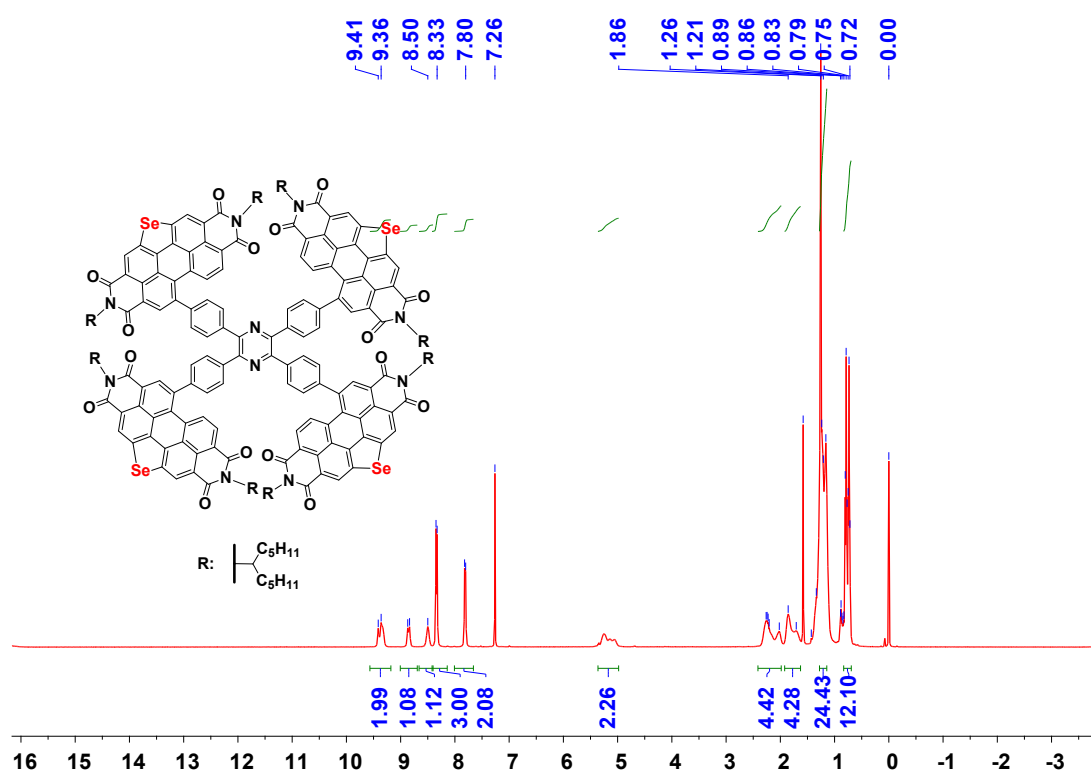


Figure S11. ^1H NMR spectrum of PPDI-Se.

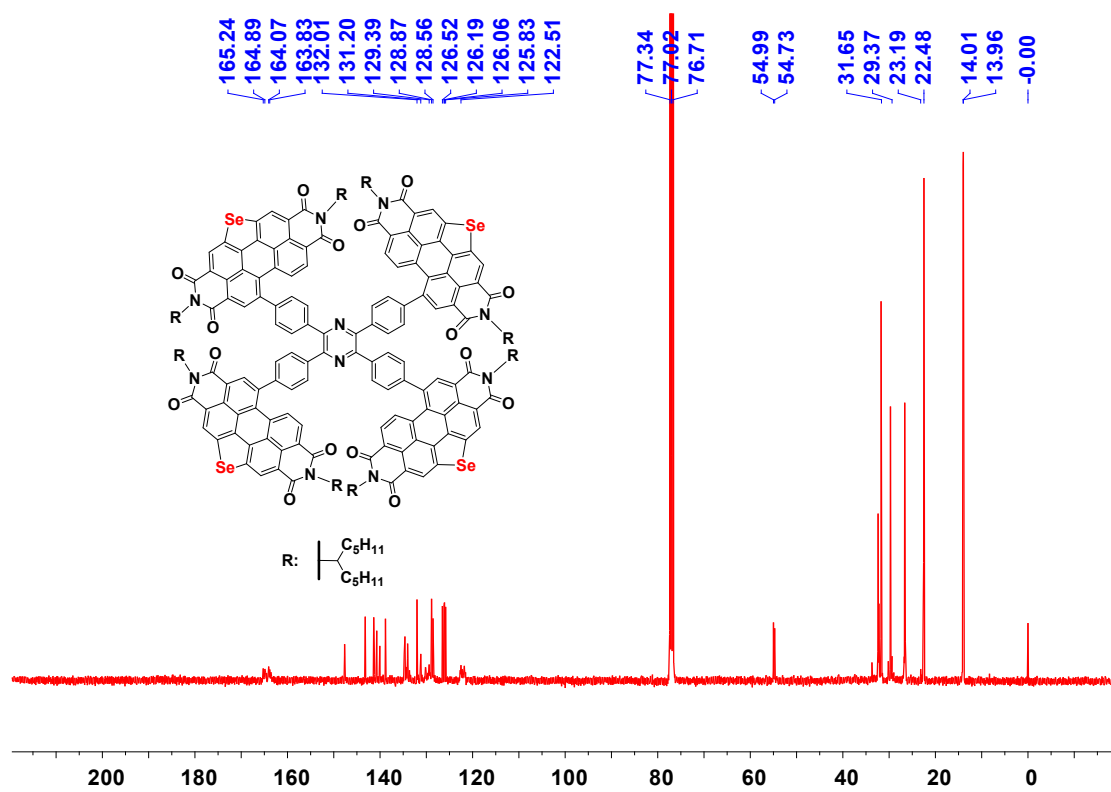


Figure S12. ^{13}C NMR spectrum of PPDI-Se.

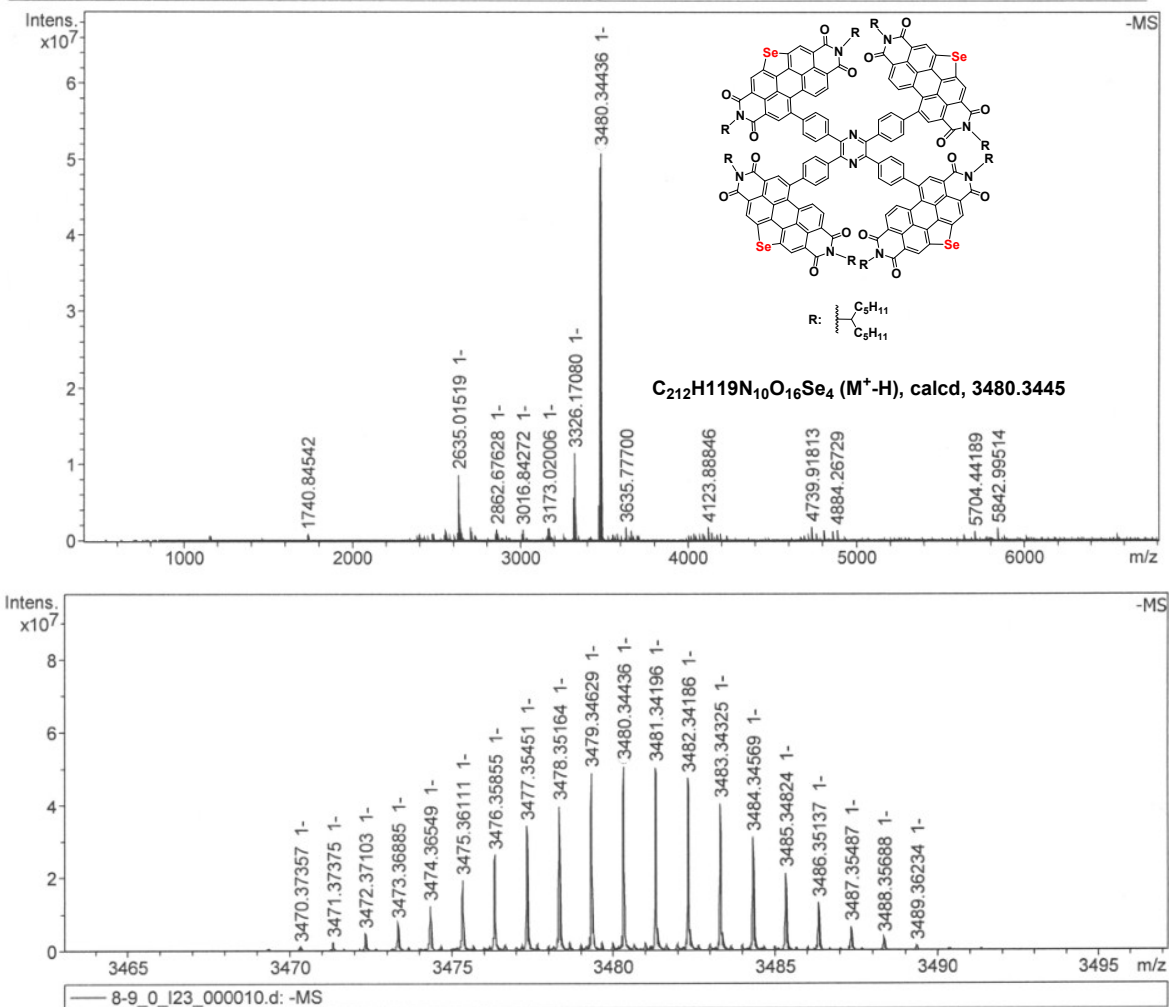
Analysis Info
 Analysis Name D:\Data\MALDI\2019\10\10\8-9_0_I23_000010.d
 Method MALDI_P_100-3000
 Sample Name MURU-N-ESI
 Comment

Acquisition Date 10/10/2019 5:28:48 PM

Operator
 Instrument solariX

Acquisition Parameter

Acquisition Mode	Single MS	Acquired Scans	3	Calibration Date	Thu Oct 10 05:21:37
Polarity	Negative	No. of Cell Fills	1	Data Acquisition Size	2099152
Broadband Low Mass	404.2 m/z	No. of Laser Shots	10	Data Processing Size	4194304
Broadband High Mass	6800.0 m/z	Laser Power	14.8 lp	Apodization	Sine-Bell Multiplication
Source Accumulation	0.001 sec	Laser Shot Frequency	0.020 sec		
Ion Accumulation Time	0.300 sec				



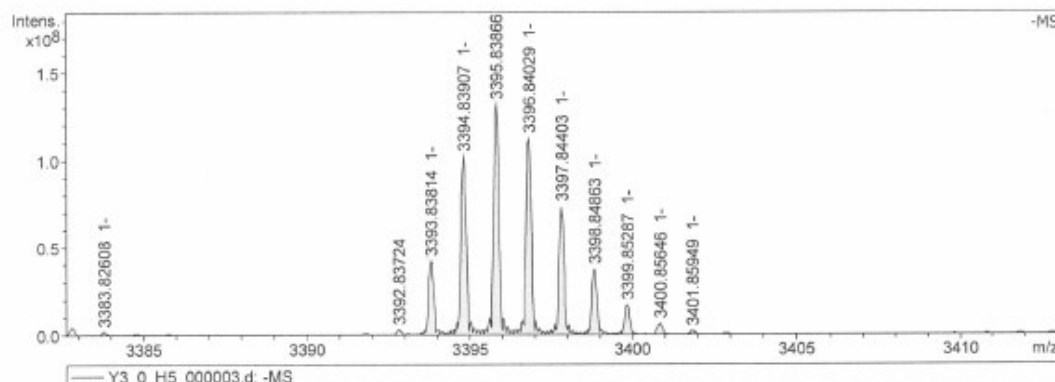
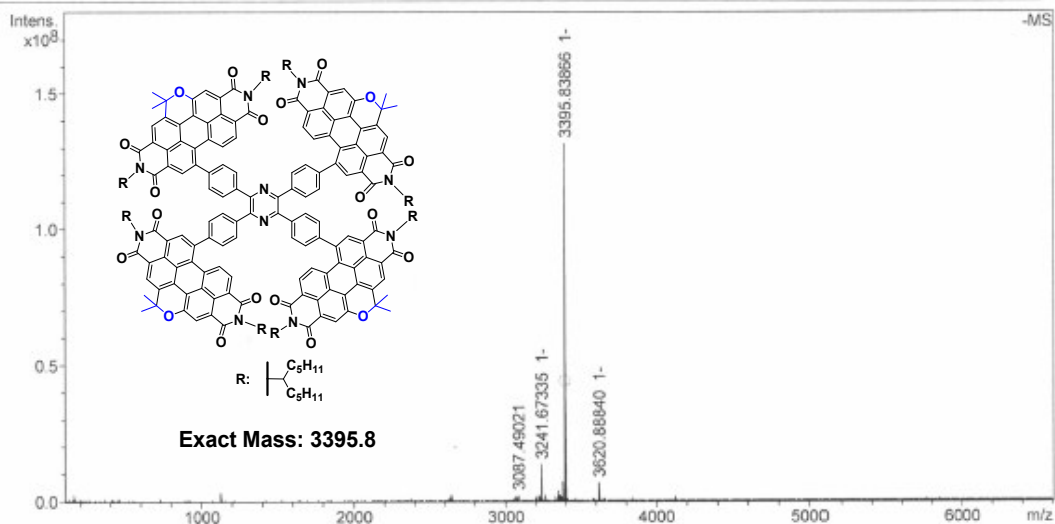
Meas. m/z	#	Ion Formula	Score	m/z	err [ppm]	Mean err [ppm]	mSigma	rdb	e ⁻ Conf	N-Rule
3480.344359	1	C ₂₁₂ H ₁₁₉ N ₁₀ O ₁₆ Se ₄	100.00	3480.34777	1.0	0.0	78.7	108.0	odd	ok

Figure S13. MALDI-TOF profile of PPDI-Se.

Analysis Info
 Analysis Name D:\Data\MALDI\2018\0930\Y3_0_H5_000003.d
 Method MALDI_P_100-3000
 Sample Name MURU-N-ESI
 Comment

Acquisition Date 9/30/2018 5:40:57 PM
 Operator
 Instrument solarix

Acquisition Parameter
 Acquisition Mode Single MS
 Polarity Negative
 Broadband Low Mass 101.1 m/z
 Broadband High Mass 6600.0 m/z
 Source Accumulation 0.001 sec
 Ion Accumulation Time 0.300 sec
 Acquired Scans 3
 No. of Cell Fills 1
 No. of Laser Shots 12
 Laser Power 43.0 lp
 Laser Shot Frequency 0.020 sec
 Calibration Date Sat Sep 29 04:54:20
 Data Acquisition Size 2088152
 Data Processing Size 4194304
 Apodization Sine-Bell Multiplication



Meas. m/z	#	Ion Formula	Score	m/z	err [ppm]	mSigma	rdb	e ⁻ Conf	N-Rule
3393.838141	1	C224H244N10O20	100.00	3393.838869	0.2	8.8	108.0	odd	ok

Figure S14. MALDI-TOF profile of PPDI-O.

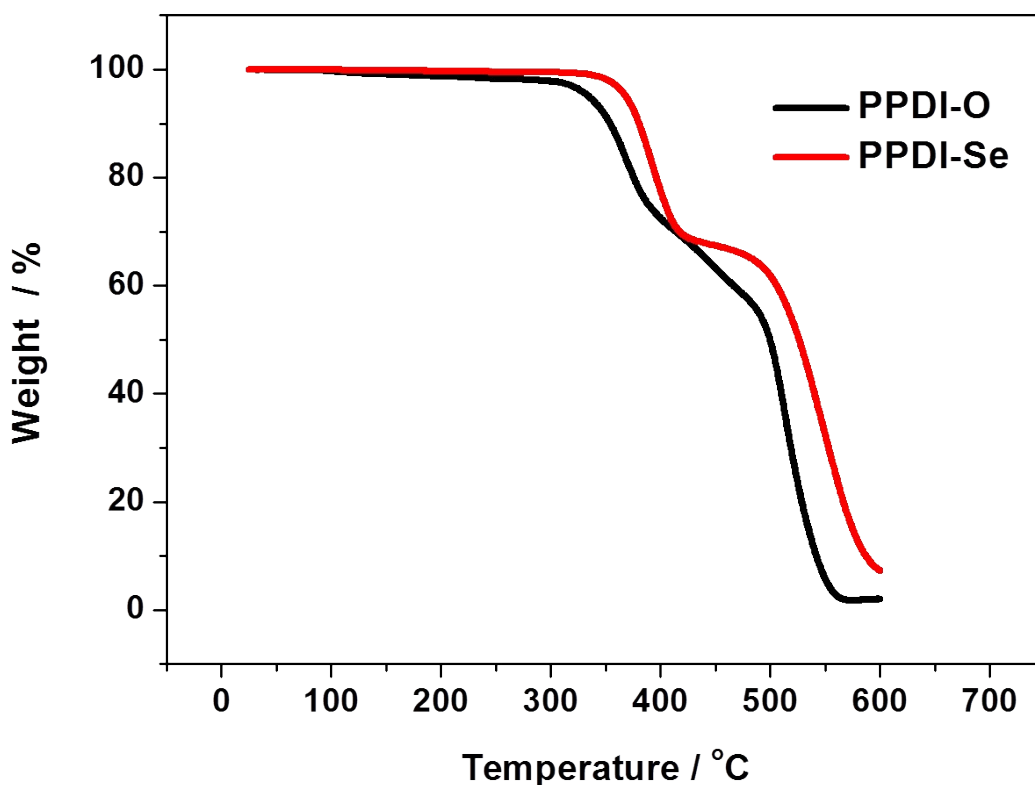


Figure S15. TGA profile of PPDI-O and PPDI-Se.

10. References

1. J. Meng, M. Gao, H. Lv and X. Zhang, *Org. Lett.*, 2015, **17**, 1842-1845.
2. H. Lin, S. Chen, H. Hu, L. Zhang, T. Ma, J. Y. Lai, Z. Li, A. Qin, X. Huang and B. Tang, *Adv. Mater.*, 2016, **28**, 8546-8551.
3. L. J. Huo, T. Liu, X. Sun, Y. Cai, A. J. Heeger and Y. Sun, *Adv. Mater.*, 2015, **27**, 2938-2944.
4. M. J. Frisch, G. W. Trucks, H. B. Schlegel, G. E. Scuseria, M. A. Robb, J. R. Cheeseman, G. Scalmani, V. Barone, G. A. Petersson, H. Nakatsuji, X. Li, M. Caricato, A. Marenich, J. Bloino, B. G. Janesko, R. Gomperts, B. Mennucci, H. P. Hratchian, J. V. Ortiz, A. F. Izmaylov, J. L. Sonnenberg, D. Williams-Young, F. Ding, F. Lipparini, F. Egidi, J. Goings, B. Peng, A. Petrone, T. Henderson, D. Ranasinghe, V. G. Zakrzewski, J. Gao, N. Rega, G. Zheng, W. Liang, M. Hada, M. Ehara, K. Toyota, R. Fukuda, J. Hasegawa, M. Ishida, T. Nakajima, Y. Honda, O. Kitao, H. Nakai, T. Vreven, K. Throssell, J. A. Montgomery, Jr., J. E. Peralta, F. Ogliaro, M. Bearpark, J. J. Heyd, E. Brothers, K. N. Kudin, V. N. Staroverov, T. Keith, R. Kobayashi, J. Normand, K. Raghavachari, A. Rendell, J. C. Burant, S. S. Iyengar, J. Tomasi, M. Cossi, J. M. Millam, M. Klene, C. Adamo, R. Cammi, J. W. Ochterski, R. L. Martin, K. Morokuma, O. Farkas, J. B. Foresman, and D. J. Fox, Gaussian 09, revision A.1; Gaussian, Inc.: Wallingford, CT, 2009.